

# Influence of annealing conditions on the optical and structural properties of spin-coated As<sub>2</sub>S<sub>3</sub> chalcogenide glass thin films

Shanshan Song, Janesha Dua, and Craig B. Arnold\*

Department of Electrical Engineering and Princeton Institute for the Science and Technology of Materials, Princeton University, Princeton, NJ 08544

[\\*cbarnold@princeton.edu](mailto:cbarnold@princeton.edu)

**Abstract:** Spin-coating of chalcogenide glass is a low-cost, scalable method to create optical grade thin films, which are ideal for visible and infrared applications. In this paper, we study the influence of annealing on optical parameters of As<sub>2</sub>S<sub>3</sub> films by examining UV-visible and infrared spectroscopy and correlating the results to changes in the physical properties associated with solvent removal. Evaporation of excess solvent results in a more highly coordinated, denser glass network with higher index and lower absorption. Depending on the annealing temperature and time, index values ranging from n=2.1 to the bulk value (n=2.4) can be obtained, enabling a pathway to materials optimization.

©2009 Optical Society of America

**OCIS codes:** (310.6860) Thin films, optical properties; (160.2750) Glass and other amorphous materials

---

## References and links

1. T. Kanamori, Y. Terunuma, S. Takahashi, and T. Miyashita, "Chalcogenide glass fibers for mid-Infrared transmission," *J. Lightwave Technol.* **2**, 607 (1984).
2. K. Petkov, and P. J. S. Ewen, "Photoinduced changes in the linear and non-linear optical properties of chalcogenide glasses," *J. Non-Cryst. Solids* **249**, 150 (1999).
3. A. E. Owen, A. P. Firth, and P. J. S. Ewen, "Photo-induced structural and physico-chemical changes in amorphous chalcogenide semiconductors," *Phil. Mag. B* **52**, 347 (1985).
4. J. M. Harbold, F. O. Ilday, F. W. Wise, J. S. Sanghera, V. Q. Nguyen, L. B. Shaw, and I. D. Aggarwal, "Highly nonlinear As-S-Se glasses for all-optical switching," *Opt. Lett.* **27**, 119 (2002).
5. A. Zoubir, M. Richardson, C. Rivero, A. Schulte, C. Lopez, and K. Richardson, "Direct femtosecond laser writing of waveguides in As<sub>2</sub>S<sub>3</sub> thin films," *Opt. Lett.* **29**, 748 (2004).
6. T. K. Sudoh, Y. Nakano, and K. Tada, "Wavelength trimming technology for multiple-wavelength distributed-feedback laser arrays by photo-induced refractive index change," *Electronics Letters* **33**, 216 (1997).
7. S. Song, S. S. Howard, Z. Liu, A. O. Dirisu, C. F. Gmachl, and C. B. Arnold, "Mode tuning of quantum cascade lasers through optical processing of chalcogenide glass claddings," *Appl. Phys. Lett.* **89**, 041115 (2006).
8. M. W. Lee, C. Grillet, C. L. C. Smith, D. J. Moss, B. J. Eggleton, D. Freeman, B. Luther-Davies, S. Madden, A. Rode, Y. Ruan, and Y. Lee, "Photosensitive post tuning of chalcogenide photonic crystal waveguides," *Optics Express* **15**, 1277 (2007).
9. K. E. Youden, T. Grevatt, R. W. Eason, H. N. Rutt, R. S. Deol, and G. Wylangowski, "Pulsed-laser deposition of Ga-La-S chalcogenide glass thin-film optical wave-guides," *Appl. Phys. Lett.* **63**, 1601 (1993).
10. V. Balan, C. Vigreux, and A. Pradel, "Chalcogenide thin films deposited by radio-frequency sputtering," *J. Optoelectronics and Advanced Materials* **6**, 875 (2004).
11. C. B. Arnold, and A. Pique, "Laser direct write processing," *MRS Bulletin* **32**, 9 (2007).
12. C. B. Arnold, P. Serra, and A. Pique, "Laser direct-write techniques for printing of complex materials," *MRS Bulletin* **32**, 23 (2007).
13. C. Tsay, E. Mujagic, C. K. Madsen, C. F. Gmachl, and C. B. Arnold, "Integrated chalcogenide waveguides with quantum cascade lasers for on-chip mid-infrared photonic circuits," submitted (2009).
14. G. C. Chern, and I. Lauks, "Spin-coated amorphous chalcogenide films," *J. Appl. Physics.* **53**, 6979 (1982).

15. B. Singh, G. C. Chern, and I. Lauks, "Application of spin-coated As<sub>2</sub>S<sub>3</sub> thin films in a high resolution trilayer resist system," *Appl. Phys. Lett.* **45**, 74 (1984).
  16. J. M. González-Leal, M. Stuchlik, M. Vlcek, R. Jiménez-Garay, and E. Márquez, "Influence of the deposition technique on the structural and optical properties of amorphous As-S films," *Applied Surface Science* **246**, 348 (2005).
  17. J. J. Santiago, M. Sano, M. Hamman, and N. Chen, "Growth and optical characterization of spin-coated As<sub>2</sub>S<sub>3</sub> multilayer thin films," *Thin Solid Films* **147**, 275 (1987).
  18. S. Shtutina, M. Klebanov, S. R. V. Lyubin, and V. Volterra, "Photoinduced phenomena in spin-coated vitreous As<sub>2</sub>S<sub>3</sub> and AsSe films," *Thin Solid Films* **261**, 263 (1995).
  19. J. Tauc, "Absorption edge and internal electric fields in amorphous semiconductors," *Materials Research Bulletin* **5**, 721 (1970).
  20. R. Swanepoel, "Determination of the thickness and optical constants of amorphous silicon," *J. Phys. E* **16**, 1214 (1983).
  21. E. Marquez, J. Ramirez-Malo, P. Villarest, R. Jimenez-Garay, P. J. S. Ewen, and A. E. Owen, "Calculation of the thickness and optical constants of amorphous arsenic sulfide films from their transmission spectra," *J. Phys. D: Appl. Phys.* **25**, 535 (1991).
  22. S. Wemple, and M. DiDomenico, "Behavior of electronic dielectric constant in covalent and ionic materials," *Phys. Rev. B* **3**, 1338 (1971).
  23. S. Wemple, "Refractive-index behavior of amorphous semiconductors and glasses," *Phys. Rev. B* **7**, 3767 (1973).
  24. G. C. Chern, I. Lauks, and A. R. McGhie, "Spin coated amorphous chalcogenide films: Thermal properties," *J. Appl. Phys.* **54**, 4596 (1983).
  25. Material Safety Data Sheet for Arsenic (III) sulfide, Fisher Scientific.
  26. S. R. Elliott, *Physics of Amorphous Materials* (Longman, London, 1990).
  27. G. C. Chern, "Spin-coated amorphous chalcogenide films, Ph.D. dissertation," University of Pennsylvania (1984).
- 

## 1. Introduction

Chalcogenide glasses have drawn great interest for their high refractive index, low-loss in mid-infrared, a wide range of photo-induced phenomena, and optical nonlinearities.[1-3] They are ideal candidates for various applications in infrared optics, such as lenses, all-optical switching, and laser written waveguides.[4, 5] In addition, the photosensitive properties of chalcogenide glasses enable optical tuning of photonic structures, such as tuning for solid-state lasers [6, 7] and photonic crystal waveguides [8].

For most applications, thin film deposition with good film quality is a prerequisite. The films are expected to have a composition similar to the bulk glass, a low surface roughness, a reproducible and controlled refractive index and low optical loss. Chalcogenide glass thin films are conventionally prepared by vacuum coating techniques (thermal evaporation or sputtering) or pulsed laser deposition.[9, 10] However, less conventional techniques such as spin-coating of glassy films from solution can have certain advantages for realizing large area or thick film deposition. Spin-coating approaches have the added advantage that the same solutions can be adopted for other precision dispensing techniques such as mold casting, ink jet or laser direct write [11-13], giving spatial control of the added material. Chern and Lauks first introduced the spin-coating deposition method of preparing chalcogenide films for high resolution photoresists.[14, 15] They demonstrated that amorphous films can be deposited from their solutions and retain many of the glass properties.

Solvent residue from solution-based deposition can introduce complications in optical properties of the thin films. A review of the literature reveals a range of optical parameters for the same material produced by different studies and different processing methods.[16, 17] Heat treatment has a major influence on the amount of organic solvent left in the thin films and therefore on the optical and structural properties of the resulting films. It is important to clarify the relationship between annealing conditions and film properties and this information is necessary for stability and optimization of optical parameters.

In this paper, we examine the influence of annealing conditions on optical properties of spin-coated As<sub>2</sub>S<sub>3</sub> films. Infrared and UV-visible transmission spectra is used to characterize

the optical properties of films subjected to annealing temperatures ranging from 60 to 180 °C and durations from 1 hour to 20 hours resulting in differing amounts of residual solvent. Results are correlated with density and thermogravimetric analysis, which provide information about the evolution of amine and other components from as-deposited films. Finally, we discuss the effects of the solvent molecules on the glass network by applying the Wemple-DiDomenico (WDD) dispersion model to the measured refractive index data.

## 2. Experimental

Solutions of As<sub>2</sub>S<sub>3</sub> are prepared by grinding bulk As<sub>2</sub>S<sub>3</sub> pieces into a fine powder and dissolved into *n*-propylamine solvent at a concentration of 0.8 mol/L. The dissolution is carried out inside a sealed glass container to prevent solvent evaporation. The dissolving process usually takes 7 days and a magnetic stirrer can be used to expedite this process. Exposure of solution to atmospheric moisture is kept to a minimum throughout the preparation procedure since water can lead to precipitate formation.[18] The solution is pipetted onto the substrate, and the substrate is spun at 1000 rpm for 30 seconds. The resulting films are soft-baked immediately after coating under vacuum at 60 °C for 1 hour to remove most of the solvent and then hard-baked at different temperatures ranging from 60 °C up to 180 °C to remove excess solvent and to further densify the glass. In this study, the investigated thin films of As<sub>2</sub>S<sub>3</sub> glass are deposited onto either silicon wafers for infrared spectroscopy and density measurement, or onto glass microscope slides for optical spectroscopy. For thermogravimetric analysis (TGA), samples are soft-baked at 45 °C for 20 hours and then removed by scraping the solid from glass substrates. TGA is carried out on a Perkin Elmer TGA 7 system. The analysis is performed on 15-20 mg samples in the range 30 to 180 °C at 1 °C/min in a nitrogen-purged atmosphere.

Density measurements are conducted using spin-coated As<sub>2</sub>S<sub>3</sub> thin films on square silicon chips. The silicon wafers are first spin-coated and then cut into 10×10 mm square chips to insure similar film thicknesses (±5%).

The infrared transmission spectra of the films are measured with a Nicolet Fourier transform infrared (FTIR) spectrometer using a cooled mercury cadmium telluride (MCT) detector with a resolution of 4 cm<sup>-1</sup>. Absorption bands associated with the solvent *n*-propylamine are examined as a function of annealing temperature and duration using this technique.

The UV-VIS transmission spectra are measured using an Ocean Optics HR4000 high-resolution spectrometer. The optical spectra of the films show a periodic variation of the transmission value as a function of wavelength. This effect is caused by the interference between multiple reflections at the two surfaces of the film, and is influenced by both the film's thickness and its refractive index at that particular wavelength. The optical band gap,  $E_g^{opt}$  is determined from the absorption coefficient values using Tauc's extrapolation in the strong absorption region [19], i.e., from the relationship  $\alpha(h\nu) = K(h\nu - E_g^{opt})^2 / h\nu$ , where  $K$  is a constant, and the optical band gap is defined as the intercept of the plot of  $(\alpha h\nu)^{1/2}$  against  $h\nu$ . Using Swanepoel's method on the transmission spectra [20, 21], the refractive index dispersion for the films are calculated.

The refractive index as a function of wavelength are analyzed on the basis of the Wemple-DiDomenico dispersion model [22, 23], which is based on the single-oscillator approach:

$$n^2(h\nu) = 1 + \frac{E_o E_d}{E_o^2 - (h\nu)^2} \quad (1)$$

where  $h$  is Planck's constant,  $h\nu$  is the photon energy,  $E_o$  is the single-oscillator energy and  $E_d$  is the dispersion energy or oscillator strength. Plotting  $(n^2-1)^{-1}$  against  $(h\nu)^2$  allows one to

determine the oscillator parameters by fitting a straight line to the experimental points. By extrapolating the fitting line towards  $h\nu = 0$ , one can obtain the static refractive index  $n(0)$ .

The WDD model also relates the dispersion energy,  $E_d$ , to other physical parameters of the material through the following empirical relationship[22, 23]:

$$E_d(\text{eV}) = \beta N_c Z_a N_e \quad (2)$$

where  $N_c$  is the effective coordination number of the cation nearest-neighbor to the anion,  $Z_a$  is the formal chemical valency of the anion,  $N_e$  is the effective number of valence electrons per anion and  $\beta$  is a two-valued constant with either an ionic or a covalent value ( $\beta_i = 0.26 \pm 0.03$  eV and  $\beta_c = 0.37 \pm 0.04$  eV, respectively). For  $\text{As}_2\text{S}_3$  being studied, it is assumed that  $Z_a = 2$ ,  $\beta = 0.37 \pm 0.04$  eV and  $N_e = 9.3$ , which is determined by the glass stoichiometry. Based on these assumptions, any difference in  $E_d$  derived by the WDD model will be likely due to the difference in  $N_c$ , the arsenic effective coordination number, which indicates the structure of the glass network.

### 3. Results and discussion

We measure the transmission spectra of the films annealed at different temperatures. In the strong absorption region, the optical band gap can be determined by Tauc's extrapolation.[19] In the weak and medium absorption region, the refractive index dispersion can be calculated using Swanepoel's method.[20, 21]

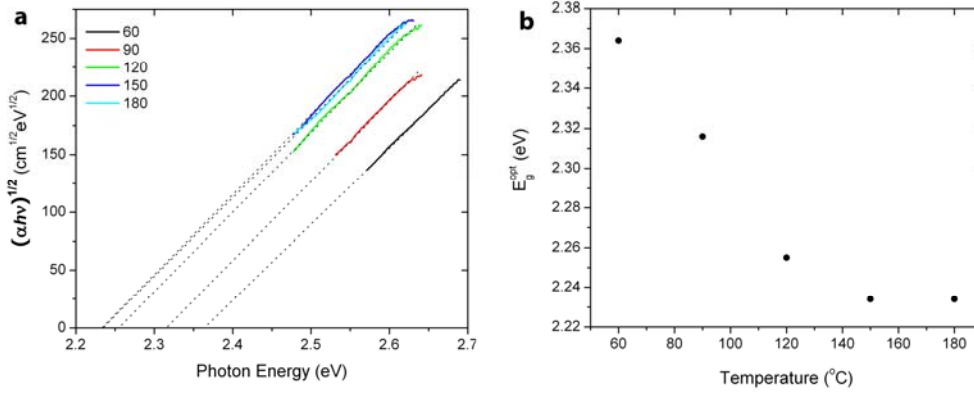


Fig. 1. Determination of optical band gap  $E_g^{\text{opt}}$  for  $\text{As}_2\text{S}_3$  films spin-coated from *n*-propylamine solutions and annealed at different temperatures for 1 hour: (a) Tauc's extrapolation, the optical band gap is defined as the intercept of the plot of  $(\alpha h\nu)^{1/2}$  against  $h\nu$ ; (b)  $E_g^{\text{opt}}$  as a function of annealing temperature.

The optical band gaps  $E_g^{\text{opt}}$  of the films as a function of the annealing temperature are determined through Tauc's extrapolation as presented in Figure 1. As expected, the annealing temperature has a significant effect on the optical band gap, with increased temperatures corresponding to a red-shift of the optical band gap.  $E_g^{\text{opt}}$  stabilizes at 2.24 eV with annealing above 150 °C. Using Swanepoel's method on the transmission spectra, the refractive index dispersion for the films are calculated and shown in Figure 2(a) and the indices at 900 nm are shown in Figure 2(b) for different annealing conditions. An increase of the annealing temperature leads to films with larger refractive indices. This behavior is consistent with the reduced optical band gap, indicating a higher relative permittivity. Furthermore, the refractive

index increases with longer annealing duration at the same temperature until saturation. The saturation index is the same for temperatures below approximately 150 °C. Above this temperature, films rapidly reach saturation at higher refractive index approaching the accepted bulk value.

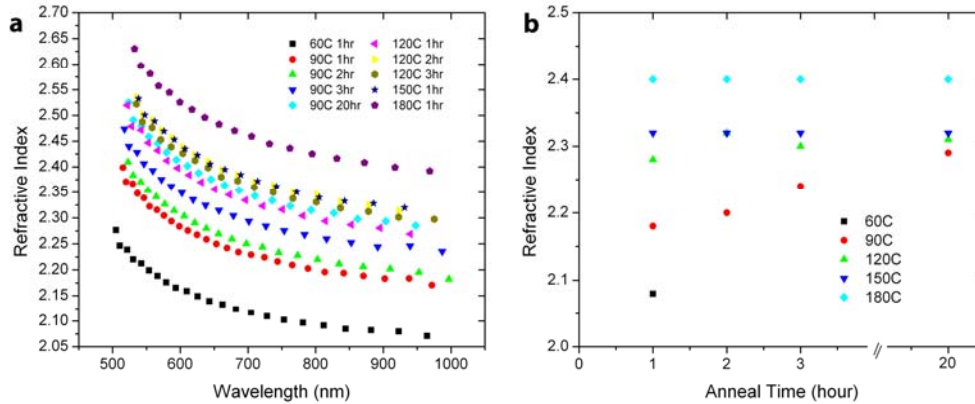


Fig. 2. (a) The refractive index dispersion for the films spin-coated from *n*-propylamine solutions and treated with different annealing conditions; (b) refractive indices at 900 nm wavelength as a function of annealing temperature and time.

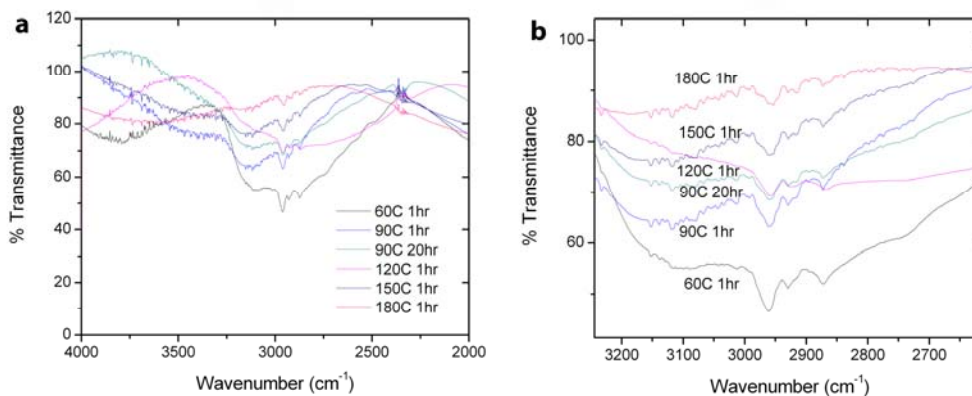


Fig. 3. Infrared transmission spectra of films spin-coated from solutions of  $As_2S_3$  in *n*-propylamine with different heat treatment: (a) Soft bake at 60 °C for 1 hour, and then thermal anneal at 60, 90, 120, 150 and 180 °C. (b) A close-up view of the spectra emphasizing the bands related to *n*-propylamine residue.

FTIR is used to verify the presence of residual solvent in the films and the effects of film annealing on optical loss in the infrared range. After spinning and soft-baking, the thin films are annealed at different temperatures for duration from 1 hour to 20 hours in order to evaporate residual *n*-propylamine in the films. The infrared transmission spectra of the resulting films are shown in Figure 3. The spectra exhibit peaks between 2290 and 2380  $cm^{-1}$ , which are related to the fluctuation of water and  $CO_2$  levels in the uncontrolled atmosphere of the measurement chamber. The FTIR spectra also show an absorption band in the 2200-3200  $cm^{-1}$  range, the intensity of which decreases as the annealing temperature and duration increases. This broad absorption band can be assigned to N-H stretch and a narrower but

stronger band between 2800-3000  $\text{cm}^{-1}$  can be assigned to aliphatic C-H stretches confirming the presence of residual solvent in the film annealed at low temperatures [24]. Annealing at higher temperature or for longer duration leads to an attenuation in these bands, indicating a decrease in the organic solvent content of the film. The films are found to be free of organic content after an annealing at 150 °C in vacuum, as indicated by the disappearance of these bands in the spectra. These films exhibit a nearly uniform transmittance of over 80% across the 2.5-5  $\mu\text{m}$  wavelength range. On the other hand, for annealing temperatures at or below 90 °C, extended duration is needed to remove the remaining solvent.

To understand the physical difference between high temperature (at or above 150 °C) and low temperature annealing, we study the evolution of different constituents from as-deposited films as a function of temperature. Thermogravimetric analysis is carried out in the range 30-180 °C at 1 °C/min in a nitrogen atmosphere, as shown in Figure 4. Three regimes of weight loss are observed. From 50-120 °C, 4.0% weight loss is found as a result of loss of amine. The sample weight remains stable in the range 120-150 °C. Above 150 °C, 2.3% weight loss is caused by  $\text{H}_2\text{S}$  evolution. According to elemental analysis, the stoichiometry of as-deposited  $\text{As}_2\text{S}_3$  is proposed to be  $\text{As}_2\text{S}_{3+x}(\text{C}_3\text{H}_7\text{NH}_3^+)_{2x}$ . [24] After low temperature annealing with removal of occluded amine, a hydrogenated arsenic sulfide  $\text{As}_2\text{S}_{3+x}\text{H}_{2x}$  is left behind. Further high temperature annealing above 150 °C leads to loss of  $\text{H}_2\text{S}$  and results in a glass containing only arsenic and sulfur.

This thermogravimetric analysis helps to explain the annealing behavior shown in figures 2 and 3. In the lower temperature regime between 50 °C and 150 °C the excess amine is evaporated from the film resulting in a lower absorption and corresponding increased index of refraction. Saturation in these properties occurs when most of the occluded amine is removed from the film. The evaporation of excess amine results in a glass with hydrogen compensated sulfur dangling bonds remaining in the amorphous network. Such bonds are stable over time but cause a decrease in the index relative to the bulk  $\text{As}_2\text{S}_3$ . Above 150 °C,  $\text{H}_2\text{S}$  evolution justifies the increase in steady-state refractive index. This decomposition removes excess hydrogen from the glass resulting in a film with a stoichiometry and properties that are more closely aligned with the bulk material.

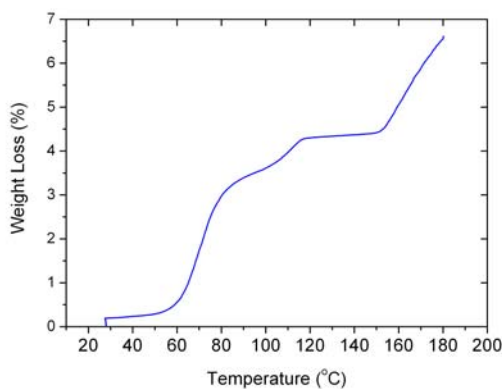


Fig. 4. Thermogravimetric analysis of  $\text{As}_2\text{S}_3$  spin-coated from *n*-propylamine solution. Sample pre-baked at 45°C for 20 hours.

**Table 1. Density of spin-coated As<sub>2</sub>S<sub>3</sub> films annealed at different annealing conditions after soft-baking**

Annealing condition	Density (g/cm <sup>3</sup> )
60 °C for 1 hr	3.0±0.3
90 °C for 1 hr	3.4±0.3
90 °C for 2 hr	3.4±0.3
90 °C for 3 hr	3.4±0.3
90 °C for 20 hr	3.5±0.3
150 °C for 1 hr	3.6±0.3
180 °C for 1 hr	3.8±0.3

Density measurements provide information about the film structure through direct characterization of the film compactness at different temperatures (Table 1). With higher annealing temperature, longer duration, and the consequent removal of solvent, the film density increases from 3.0 to 3.8 g/cm<sup>3</sup>. The density of the spin-coated films annealed at 150 °C for 1 hour or at 90 °C for 20 hours agrees with the reported value for bulk As<sub>2</sub>S<sub>3</sub> glass within the error of the measurement [25].

$$\frac{n^2 - 1}{n^2 + 2} = K\rho \quad (3)$$

$$\frac{\Delta n}{n} = \frac{6n}{(n^2 - 1)(n^2 + 2)} \frac{\Delta\rho}{\rho} \quad (4)$$

According to Lorentz-Lorenz relation, the refractive index  $n$  is related to the density of a dielectric through Eq. (3), where the constant  $K$  depends on the polarizability of the molecules constituting the dielectric. Therefore, any change in the density will lead to a change in the refractive index, as described by Eq. (4).

An increase of about 27% in density in annealed films would account for an increase of approximately 15% in refractive index, according to Eq. (4). This prediction agrees with the refractive indices at long wavelength calculated from UV-visible transmission spectra, as shown in Figure 2.

To further probe the structure of the spin coated glass network, we apply the Wemple-DiDomenico (WDD) model to refractive index dispersion calculated by Swanepoel's method. According to Eq. (1), we plot  $(n^2-1)^{-1}$  against  $(h\nu)^2$  and make least-square linear fits to the experimental points, as shown in Figure 5. The intercept on the  $(n^2-1)^{-1}$  axis gives the static refractive index  $n(0)$  while  $E_o$  and  $E_d$  could be derived from the intercept on the  $(h\nu)^2$  axis and the slope of the linear line. Table 2 lists the values of the dispersion parameters for the films with different annealing conditions, as well as the values for  $n(0)$ . As shown in Table 2, the static refractive index follows the same trend as the refractive index measured at 900 nm and increases with higher temperature and longer duration of annealing.

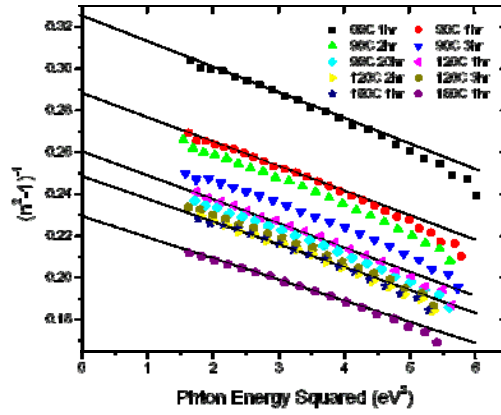


Fig. 5. Plot of refractive index factor  $(n^2-1)^{-1}$  vs.  $(h\nu)^2$  for  $\text{As}_2\text{S}_3$  films prepared by spin-coating and different heat treatment. As expected, the experimental dispersion of the refractive index departs from the linear behavior given by Eq. (1) for photon energies outside the transparent region.[22, 23]

**Table 2.** Values of static refractive indices,  $n(0)$ , WDD dispersion parameters,  $E_o$  and  $E_d$ , and As effective coordination number,  $N_c$ , for  $\text{As}_2\text{S}_3$  films prepared by spin-coating and different heat treatment

Temperature (°C)	Time (hr)	$n(0)$ ( $\pm 0.01$ )	$E_o$ (eV) ( $\pm 0.05$ )	$E_d$ (eV) ( $\pm 0.03$ )	$N_c$ ( $\pm 0.3$ )
60	1	2.02	5.16	15.89	2.3
90	1	2.11	4.95	17.17	2.5
90	2	2.13	4.86	17.14	2.5
90	3	2.18	4.96	18.48	2.7
90	20	2.21	4.77	18.58	2.7
120	1	2.20	4.75	18.20	2.6
120	2	2.24	4.69	18.75	2.7
120	3	2.23	4.74	18.73	2.7
120	20	2.23	4.74	18.73	2.7
150	1	2.24	4.78	19.21	2.8
150	20	2.24	4.78	19.21	2.8
180	1	2.32	4.78	20.87	3.0

According to Eq. (2), any difference in  $E_d$  will be likely due to the difference in the As effective coordination number,  $N_c$ , since we assume that  $\beta$ ,  $Z_a$  and  $N_c$  are constant. As reported [26], the glass network of  $\text{As}_2\text{S}_3$  consists of locally two-dimensional structural layers, formed by  $\text{AsS}_3$  pyramidal units linked through a common two-fold coordinated S, and interacting with each other by weak intermolecular bonds. Therefore,  $N_c > 3$  can be expected as a result of those As atoms acting as bonding points between layers. The As effective coordination number  $N_c$  for bulk  $\text{As}_2\text{S}_3$  glass is reported to be 3.2.[23] However, as shown in Table 2, the calculated  $N_c$  for spin-coated  $\text{As}_2\text{S}_3$  films is lower than 3.0, depending on the annealing condition.  $N_c$  increases with higher temperature and longer duration of annealing and ranges from 2.3 to 3.0. This low  $N_c$  is a result of solvent and hydrogen remaining in the material, and different amorphous structure in spin-coated films as compared to melted, bulk glass. Chern et al. [27] showed that solvent molecules are linked to S atoms through the  $-\text{NH}_2$  amine radical.

The solvent molecules in the glass matrix break the continuous random network model expected for these films and contribute to increase the structural randomness in the spin-coated films and fill in the voids around the  $\text{AsS}_3$  pyramidal units. There is a weaker interaction between structural layers forming the amorphous network in the spin-coated films than in bulk glass, causing the lower  $N_c$  observed. Above 150 °C the solvent is fully removed and the change in coordination is associated with the removal of hydrogen from the glass network resulting in a greater interaction between structural units.

#### **4. Conclusions**

In this paper, we examine the influence of annealing conditions on optical properties of spin-coated  $\text{As}_2\text{S}_3$  thin films, by analyzing refractive index dispersion, optical band gap and absorption in infrared. Optical parameters are closely related to the amount of solvent residue, film density and glass structural network. For films annealed in the low temperature regime (< 150 °C) the evolution of excess solvent enables one to select any desired index with the range of 2.1-2.3 by controlling the duration of the anneal. Above this temperature regime, there is a structural change in the amorphous material associated with the removal of hydrogen from the glass network leading to a film with a higher index (2.3-2.4) that is comparable to bulk  $\text{As}_2\text{S}_3$ .

#### **Acknowledgement**

This work is supported by the National Science Foundation under Grant No. EEC-0540832. The authors also wish to thank K. Richardson for valuable discussion.